Dissection of Filamentous Growth by Transposon Mutagenesis in *Saccharomyces cerevisiae*

Hans-Ulrich Mösch and Gerald R. Fink*

*Institute for Microbiology, Georg-August-University Göttingen, D-37077 Göttingen, Germany and *Whitehead Institute for Biomedical Research and Department of Biology, Massachusetts Institute of Technology, Cambridge, Massachusetts 02142*

Manuscript received September 12, 1996
Accepted for publication December 5, 1996

ABSTRACT

Diploid *Saccharomyces cerevisiae* strains starved for nitrogen undergo a developmental transition from growth as single yeast form (YF) cells to a multicellular form consisting of filaments of pseudohyphal (PH) cells. Filamentous growth is regulated by an evolutionarily conserved signaling pathway that includes the small GTP-binding proteins Ras2p and Cdc42p, the protein kinases Ste20p, Ste11p and Ste7p, and the transcription factor Ste12p. Here, we designed a genetic screen for mutant strains defective for filamentous growth (*dfg*) to identify novel targets of the filamentation signaling pathway, and we thereby identified 16 different genes, *CDC39, STE12, TEC1, WHI3, NAB1, DBR1, CDC55, SRV2, TPM1, SPA2, BNI1, DFG5, DFG9, DFG10, BUD8* and *DFG16*, mutations that block filamentous growth. Phenotypic analysis of *dfg* mutant strains genetically dissects filamentous growth into the cellular processes of signal transduction, bud site selection, cell morphogenesis and invasive growth. Epistasis tests between *dfg* mutant alleles and dominant activated alleles of the *RAS2* and *STE11* genes, $RAS2^{Val19}$ and *STE11-4*, respectively, identify putative targets for the filamentation signaling pathway. Several of the genes described here have homologues in filamentous fungi, where they also regulate fungal development.

THE baker's yeast, *Saccharomyces cerevisiae*, is a dimorphic fungus that interconverts between multicellular filamentous and unicellular growth modes (GIMENO and FINK 1992, 1994; GIMENO *et al.* 1992). When starved for nitrogen, *MAT***a**/*MAT*α diploid strains of *S. cerevisiae* switch from growth as individual ellipsoidal cells, called yeast form (YF) cells, to chains of elongated cells, called pseudohyphae (PH). An ellipsoidal YF mother cell enters the filamentous growth phase by dividing to produce an elongated PH daughter cell. This PH cell in turn produces PH daughter cells that remain connected to the mother, leading to the pseudohyphal filaments. The switch from YF to PH growth is accompanied by changes in at least four different cellular processes. (1) Bud site selection of cells changes from bipolar to unipolar, resulting in linear filamentous chains of cells. (2) Cell morphogenesis is altered from ellipsoidal-shaped YF cells to long thin PH cells. (3) Cell separation switches from complete to incomplete scission, so that cells remain attached to each other. (4) PH cells, in contrast to YF cells, exhibit invasive growth behavior, resulting in invasion of the agar. Therefore, yeast and PH forms of diploid *S. cerevisiae* are distinct cell types each with a unique budding pattern, cell shape, invasive growth behavior, and cell cycle (GIMENO *et al.* 1992; KRON *et al.* 1994).

Pseudohyphal growth of *S. cerevisiae* exhibits features common to filamentous growth of pathogenic fungi, where the dimorphic transition is thought to be critical for pathogenicity (SHEPHERD 1988). The most frequently isolated human fungal pathogen, *Candida albicans*, can switch from growth as budding YF cells to growth as filamentous hyphae. This switch is thought to be of particular significance for invasion of an immunocompromised host (ODDS 1987, 1992). The plant pathogen *Ustilago maydis*, the causitive agent for corn smut, is pathogenic only in its filamentous form (SCHULZ *et al.* 1990; BANUETT 1992). Thus, studies of *S. cerevisiae* dimorphism aided by the power of genetics in this organism may reveal principles of dimorphism common to all fungi.

In *S. cerevisiae*, a number of regulatory genes have been identified that control filamentous growth. They include the genes encoding the small GTP-binding proteins Ras2p (GIMENO *et al.* 1992) and Cdc42p (MÖSCH *et al.* 1996), the protein kinases Ste20p (a homologue of mammalian $p65^{PAK}$ protein kinases), Ste11p (a MEKK or MEK kinase), Ste7p (a MEK or MAPK kinase), and the transcription factor Ste12p (LIU *et al.* 1993). Filamentous growth is regulated by an evolutionarily conserved signaling pathway where Ras2p signals via the Cdc42p/Ste20p/MAPK module (MÖSCH *et al.* 1996). In addition, several other genes have been reported that function as inducers or inhibitors of filamentous growth (LJUNGDAHL *et al.* 1992; BLACKETER *et al.* 1993; GIMENO and FINK 1994). However, the role of these genes in the filamentous growth signaling pathway remains to be determined.

Remarkably, most of the genes that have been found

Corresponding author: Gerald R. Fink, Whitehead Institute for Biomedical Research, Nine Cambridge Center, Cambridge, MA 02142.

TABLE 1

Yeast strains

Strain	Genotype	Source
L5526	*MAT***a** *ura3-52 trp1::hisG*	G. R. FINK
L5527	*MATα ura3-52 trp1::hisG*	G. R. FINK
10480-2C	*MATα ura3-52 leu2::hisG*	G. R. FINK
10511-9D	*MAT***a** *ura3-52 leu2::his G trp1::hisG*	G. R. FINK
HMY15-33	*MAT***a** *cdc39-100 ura3-52 leu2::hisG trp1::hisG*	This study
HMY15-248	*MAT***a** *ste12-101 ura3-52 leu2::hisG trp1::hisG*	This study
HMY15-64	*MAT***a** *whi3-100 ura3-52 leu2::hisG trp1::hisG*	This study
HMC203	*MAT***a**/*MATα cdc39-100/cdc39-100 ura3-52/ura3-52 leu2::hisG/leu2::hisG trp1::hisG/TRP1*	This study
HMC204	*MAT***a**/*MATα cdc39-100/CDC39 ura3-52/ura3-52 leu2::hisG/leu2::hisG trp1::hisG/TRP1*	This study
L5427	*MAT***a**/*MATα ste12::LEU2/ste12::LEU2 ura3-52/ura3-52 leu2::hisG/leu2::hisG*	G. R. FINK
HMC267	*MAT***a**/*MATα tec1-101/tec1-101 ura3-52/ura3-52 leu2::hisG/leu2::hisG trp1::hisG/TRP1*	This study
HMC268	*MAT***a**/*MATα tec1-101/TEC1 ura3-52/ura3-52 leu2::hisG/leu2::hisG trp1::hisG/TRP1*	This study
HMC233	*MAT***a**/*MATα whi3-100/whi3-100 ura3-52/ura3-52 leu2::hisG/leu2::hisG trp1::hisG/TRP1*	This study
HMC234	*MAT***a**/*MATα whi3-100/WHI3 ura3-52/ura3-52 leu2::hisG/leu2::hisG trp1::hisG/TRP1*	This study
HMC275	*MAT***a**/*MATα nab1-100/nab1-100 ura3-52/ura3-52 leu2::hisG/leu2::hisG trp1::hisG/TRP1*	This study
HMC276	*MAT***a**/*MATα nab1-100/NAB1 ura3-52/ura3-52 leu2::hisG/leu2::hisG trp1::hisG/TRP1*	This study
HMC237	*MAT***a**/*MATα dbr1-100/dbr1-100 ura3-52/ura3-52 leu2::hisG/leu2::hisG trp1::hisG/TRP1*	This study
HMC238	*MAT***a**/*MATα dbr1-100/DBR1 ura3-52/ura3-52 leu2::hisG/leu2::hisG trp1::hisG/TRP1*	This study
HMC199	*MAT***a**/*MATα cdc55-100/cdc55-100 ura3-52/ura3-52 leu2::hisG/leu2::hisG trp1::hisG/TRP1*	This study
HMC200	*MAT***a**/*MATα cdc55-100/CDC55 ura3-52/ura3-52 leu2::hisG/leu2::hisG trp1::hisG/TRP1*	This study
HMC205	*MAT***a**/*MATα srv2-100/srv2-100 ura3-52/ura3-52 leu2::hisG/leu2::hisG trp1::hisG/TRP1*	This study
HMC206	*MAT***a**/*MATα srv2-100/SRV2 ura3-52/ura3-52 leu2::hisG/leu2::hisG trp1::hisG/TRP1*	This study
HMC281	*MAT***a**/*MATα tpm1-100/tpm1-100 ura3-52/ura3-52 leu2::hisG/leu2::hisG trp1::hisG/TRP1*	This study
HMC282	*MAT***a**/*MATα tpm1-100/TPM1 ura3-52/ura3-52 leu2::hisG/leu2::hisG trp1::hisG/TRP1*	This study
HMC245	*MAT***a**/*MATα spa2-100/spa2-100 ura3-52/ura3-52 leu2::hisG/leu2::hisG trp1::hisG/TRP1*	This study
HMC246	*MAT***a**/*MATα spa2-100/SPA2 ura3-52/ura3-52 leu2::hisG/leu2::hisG trp1::hisG/TRP1*	This study
HMC283	*MAT***a**/*MATα bni1-100/bni1-100 ura3-52/ura3-52 leu2::hisG/leu2::hisG trp1::hisG/TRP1*	This study
HMC284	*MAT***a**/*MATα bni1-100/BNI1 ura3-52/ura3-52 leu2::hisG/leu2::hisG trp1::hisG/TRP1*	This study
HMC235	*MAT***a**/*MATα dfg5-100/dfg5-100 ura3-52/ura3-52 leu2::hisG/leu2::hisG trp1::hisG/TRP1*	This study
HMC236	*MAT***a**/*MATα dfg5-100/DFG5 ura3-52/ura3-52 leu2::hisG/leu2::hisG trp1::hisG/TRP1*	This study
HMC263	*MAT***a**/*MATα dfg9-100/dfg9-100 ura3-52/ura3-52 leu2::hisG/leu2::hisG trp1::hisG/TRP1*	This study
HMC264	*MAT***a**/*MATα dfg9-100/DFG9 ura3-52/ura3-52 leu2::hisG/leu2::hisG trp1::hisG/TRP1*	This study
HMC239	*MAT***a**/*MATα dfg10-100/dfg10-100 ura3-52/ura3-52 leu2::hisG/leu2::hisG trp1::hisG/TRP1*	This study
HMC240	*MAT***a**/*MATα dfg10-100/DFG10 ura3-52/ura3-52 leu2::hisG/leu2::hisG trp1::hisG/TRP1*	This study
HMC209	*MAT***a**/*MATα bud8-108/bud8-108 ura3-52/ura3-52 leu2::hisG/leu2::hisG trp1::hisG/TRP1*	This study
HMC210	*MAT***a**/*MATα bud8-108/BUD8 ura3-52/ura3-52 leu2::hisG/leu2::hisG trp1::hisG/TRP1*	This study
HMC225	*MAT***a**/*MATα dfg16-100/dfg16-100 ura3-52/ura3-52 leu2::hisG/leu2::hisG trp1::hisG/TRP1*	This study
HMC226	*MAT***a**/*MATα dfg16-100/DFG16 ura3-52/ura3-52 leu2::hisG/leu2::hisG trp1::hisG/TRP1*	This study
L5366	*MAT***a**/*MATα ura3-52/ura3-52*	G. R. FINK

so far to affect filamentous growth encode proteins involved in signal transduction. None of the targets for this signaling pathway is known. Therefore, we designed a general screen for the isolation of genes required for filamentous growth in *S. cerevisiae*. Mutations in 16 genes (*CDC39, STE12, TEC1, WHI3, NAB1, DBR1, CDC55, SRV2, TPM1, SPA2, BNI1, DFG5, DFG9, DFG10, BUD8* and *DFG16*) were found to suppress filamentous growth. Analysis of these mutations indicates that invasion can be separated from filament formation-unipolar growth, cell morphogenesis and cell separation.

MATERIALS AND METHODS

Yeast strains, media, and genetic methods: All yeast strains used in this study are described in Table 1, and are derived from Σ1278b or have been crossed into the Σ1278b genetic background (GRENSON *et al.* 1966; LIU *et al.* 1993). Standard yeast culture medium was prepared essentially as described (SHERMAN *et al.* 1986). Low ammonia medium (SLAD) for scoring pseudohyphal growth was prepared as described (GIMENO *et al.* 1992). When required, uracil was added to SLAD medium to a final concentration of 0.2 mM to make SLAD +Ura. Crosses, sporulation and tetrad dissection were performed according to SHERMAN *et al.* (1986). Yeast transformations were performed as previously described (ITO *et al.* 1983; GIETZ *et al.* 1992).

Isolation of and genetic analysis of *dfg* mutants: Mutagenesis for the isolation of *dfg* mutants was performed by using the *Tn3* transposon mutagenized yeast genomic DNA library constructed by BURNS *et al.* (1994). Strain 10511-9D (*MAT***a** *ura3-52 leu2::hisG trp1::hisG*) carrying both plasmids B2185 and B3364 was transformed with *Not*I-cleaved DNA from 14 different pools of the yeast genomic library carrying random *Tn3::lacZ::LEU2* insertions (BURNS *et al.* 1994), according to the protocol of GIETZ *et al.* (1992). Approximately 280,000 transformants were obtained by growth selection on SC −Leu

TABLE 2

Plasmids

Plasmid	Description	Source
pRS316	*URA3*-marked centromere vector	SIKORKSI and HIETER (1989)
pRS202	*URA3*-marked 2 μm vector	C. CONNELLY and P. HIETER
YEplac112	*TRP1*-marked 2 μm vector	GIETZ and SUGINO (1988)
B2185	4.4-kb fragment containing the *MATα* locus in pRS316	FINK laboratory collection
B3364	2.6-kb fragment containing *PHD1* in YEplac112	FINK laboratory collection
pCG38	2.6-kb fragment containing *PHD1* in pRS202	GIMENO and FINK (1994)
B2065	*GAL1,10::STE12* in *URA3* marked 2 μm vector	B. ERREDE
B2616	5.6-kb fragment containing *STE11-4* in YCp50	G. SPRAGUE
B2255	$RAS2^{Val19}$ in YCp50	M. WIGLER
B3366	6.5-kb fragment containing *TEC1* in pRS202	This study

−Trp −Ura medium and collected as a pool. Cells from this pool were washed with water and plated on SLAD medium at a density of ~1000 colonies per plate, and 100,000 colonies were visually screened for *dfg* mutant strains by using a Wild M5A stereomicroscope with a transmitted light console base.

Four hundred twenty-four putative *dfg* mutants were picked and further analyzed by a qualitative filamentous growth assay, revealing 56 Dfg^- strains that exhibited severe defects in filamentous growth. Segregants that had lost the plasmids carrying *PHD1* and the *MATα* locus were isolated from each of these 56 putative mutants. These segregants were crossed to strain 10480-2C (*MATα ura3-52 leu2::hisG*). Five out of 56 Dfg^- strains were sterile and were directly analyzed by rescue of the genomic DNA immediately adjacent to the *LEU2* insertion responsible for the mutation. The remaining 51 Dfg^- strains were further analyzed by tetrad analysis. For each cross between tester strain 10480-2C (*MATα ura3-52 leu2::hisG*) and these 51 Dfg^- strains (*MAT***a** *ura3-52 leu2::hisG trp1::hisG dfg::LEU2*), at least six four-spore tetrads were analyzed for growth on SC −Leu and on SC −Trp medium. In 50 out of 51 crosses, both the *LEU2* as well as the *TRP1* marker genes segregated in a 2:2 pattern in all four-spore tetrads that were analyzed, indicating that 50 of the original *dfg* mutants were carrying only a single transposon insertion. Linkage of the *dfg* mutation to the insertion was tested by intercrossing spores from the tetrads of each cross. Diploid strains either homozygous or heterozygous for the *LEU2* marker gene were constructed using a total of four different Leu^+ and two different Leu^- spore clones, and tested for filamentous growth. We made the tentative assessment of linkage if all the *LEU2/LEU2* diploids failed to filament and all the *leu2/leu2* diploids filamented. The *LEU2* marker from the insertion segment and a filamentous growth defect were genetically linked in 45 *dfg* mutants. In the remaining five Dfg^- strains, the *dfg* mutations were not linked to the *LEU2* marker gene and were not analyzed further. Genomic DNA flanking the *LEU2* insertion was isolated from each of the remaining 45 *dfg* mutants and analyzed by sequencing, revealing at least 35 independent transposon insertions in a total of 16 genes. For genes in which we isolated only one transposon insertional allele (*CDC39, NAB1, DBR1, CDC55, TPM1, SPA2, BNI1, DFG9, DFG10* and *DFG16*), we intercrossed several more meiotic progeny and tested for filamentous growth. In all these cases the data were consistent with linkage between the transposon insertion and the Dfg^- phenotype.

Plasmid rescue and DNA analysis: Genomic DNA immediately adjacent to *Tn3::lacZ::LEU2* in the *dfg* mutants was cloned essentially as described earlier (BURNS *et al.* 1994). DNA and protein homology searches were performed at the National Center for Biotechnology Information using the BLAST network service (ALTSCHUL *et al.* 1990).

Qualitative filamentous growth assay: The qualitative growth assay for filament formation was performed as described previously (GIMENO *et al.* 1992; GIMENO and FINK 1994). Strains to be tested were streaked to obtain single cells on fresh SLAD or SLAD +Ura plates. Four to six strains were streaked per plate. The streaking technique was chosen as to produce a gradient of colony density, with the highest density existing in the center of the plate. Cultures were grown at 30°, and after the appropriate period of time, representative colonies were photographed.

Determination of substrate invasion: Substrate invasion was performed first by streaking strains on SLAD plates as described above, and subsequent incubation of the plates at 30° for 3 days. Cells that had not invaded the agar were washed away by rubbing the plate with a gloved hand while rinsing the plate under running water. Cells that had invaded the agar remained as visible colonies on the surface of the washed plate. Invasiveness was confirmed by microscopic examination of the remaining cells and determination that both the plane of focus required for cell visualization resided inside the agar and that a micromanipulation needle was required to penetrate the agar to reach the cells. Invasiveness of different strains was quantified by determining the percentage of single colonies (typically 50 colonies from a streak), where a significant amount of cells remained in the agar after washing. Five different classes for invasiveness were defined: ++++, >90% colonies had cells in agar; +++, 70–90%; ++, 30–70%; +, 5–30%; −, <5%.

Determination of cell shape: Cell shape determination was performed based on a method for characterization of cell shape in *Candida albicans* (MERSON-DAVIES and ODDS 1989). After 3 days growth on SLAD medium at 30°, cells that had not invaded the agar were removed by washing the plates. Cells that had invaded the agar were scraped out with a toothpick, suspended in 50 μl of water, and analyzed for cell shape by light microscopy. Cell shape patterns of different strains were quantified by determining the length to width (l/w) ratio of 200 cells and dividing them into three different classes: round yeast form cells (round YF) with a l/w ratio of 1, oval YF cells (oval YF) with a l/w ratio between 1 and 2, long pseudohyphal cells (long PH) with a l/w ratio of >2. Numbers in the tables represent the percentage of cells in each class. The l/w ratios of large numbers of cells (>20) were estimated by eye, whereby the three different classes of cell shapes were easy to distinguish from one another. Moreover, photomicroscopy and measurement of cell dimensions of a few selected cells in each class agreed with the division in the three categories.

Bud scar staining: Cells in exponential growth phase in liquid were prepared by incubating cells in YPD medium on a roller drum at 30° until the culture reached OD_{600} 0.6. Cell suspensions were fixed at room temperature for 2 hr in 3.7% formaldehyde. Samples were rinsed twice in water and resuspended in 200 ml of a fresh stock of 1 mg/ml calcofluor white (Fluorescent Brightener #28 F6259 Sigma) in water. Samples were stained at room temperature in the dark for 10 min, and washed three times in water before observation. Bud scars were visualized by fluorescence microscopy on a Zeiss Axioskop and photographed with a 35-mm camera using TMAX 400 film (Kodak). Cells with two to 10 obvious bud scars were divided into three classes based upon bud scar distribution: bipolar, cells with two or more bud scars with at least one scar at each end of the cell (the birth end and the free end); unipolar, cells with all bud scars at one end of the cell immediately adjacent to one another; random, cells with bud scar distributions other than bipolar or unipolar. Numbers in the tables represent the percentage of cells in each class for a sample of 200 cells.

Light microscopy techniques: Light microscopy of microcolonies was performed with a Zeiss WL light microscope using bright field optics. Petri plates were placed directly on the microscope stage. To visualize the colonies, 16× and 10× long working distance objectives (Zeiss) were used. Colonies were photographed with a 35-mm camera using Technical Pan (Kodak) film. For cell shape determination, samples of invasive cells were prepared as described above, and viewed with a Zeiss WL light microscope (40× short working distance objective) using a hematocytometer (Improved Neubauer). Light photomicroscopy of invasive cells was performed by placing the cells on a slide with coverslip and viewing with Nomarski optics on a Zeiss Axioskop with a 100× objective. Photographs were taken with a 35-mm camera using Technical Pan (Kodak) film. Images were printed onto photographic paper and cell dimensions were measured directly. Length was measured along the longest axis of each cell, and width was measured at the midpoint of the longest axis (GIMENO *et al.* 1992).

Time-lapse microscopy: Bud site selection of growing filaments was determined by using a chamber for high magnification imaging of yeast growth as described previously (KRON *et al.* 1994), and viewed with a Zeiss WL light microscope using a 40× short working distance objective. Budding was observed and classified according to the site where the first bud of a virgin mother emerged. None of the cells present in the chamber (typically 10 individual cells) at time zero was scored, as their birth end could not always be determined. Instead, buds that emerged after the first time point and subsequently initiated buds of their own were defined as virgin mothers. The birth end of a virgin mother was defined as the region adjacent to the site where she was attached to her mother, and the free end was defined as the end of the cell opposite the birth end (FREIFELDER 1960). The position of bud site emergence of these virgin mothers was determined by direct microscopic observation.

RESULTS

A haploid strain that forms filaments: Recessive mutations that affect filamentation are difficult to isolate because filamentation on low ammonium medium (SLAD) is a colony phenotype that is restricted to diploids (GIMENO *et al.* 1992); haploids do not form visible filaments on this medium. Although haploid colonies exhibit invasive growth behavior with many similarities

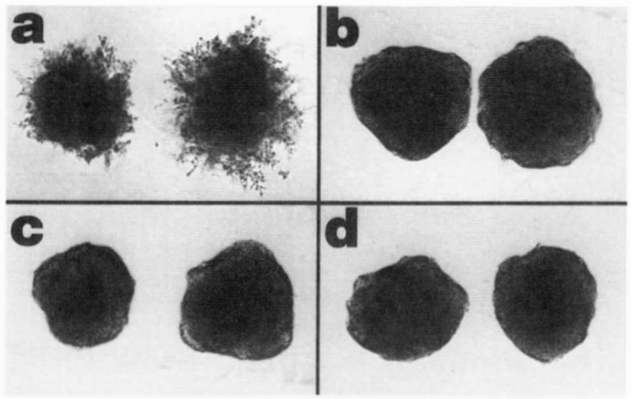

FIGURE 1.—*MAT***a**/*MATα* haploid cells overexpressing *PHD1* display filamentous growth. Strains L5526 (*MAT***a** *ura3-52 trp1::hisG*), carrying plasmids B3364 (*PHD1* on 2 μM) and B2185 (*MATα* locus in pRS316) (a); L5526, carrying plasmids B3364 and pRS316 (b); L5527 (*MATα ura3-52 trp1::hisG*), carrying B3364 and B2185 (c); and L5527, carrying B3364 and pRS316 (d), were patched on SC −Ura −Trp medium, grown overnight at 30°, and streaked to obtain single cells on nitrogen starvation (SLAD) medium. Plates were incubated at 30° and representative colonies were photographed after 72 hr of growth.

to the pseudohyphal growth of *MAT***a**/*MATα* diploid strains (ROBERTS and FINK 1994), haploid invasive growth occurs beneath the colony and does not lead to visible filaments protruding from the colony. To circumvent this problem, we tested whether *MAT***a**/*MATα* haploid strains, containing the extra copy of the opposite mating type locus on a plasmid, give sufficient filamentation to permit the isolation of *dfg*$^-$ mutations. Unfortunately, such *MAT***a**/*MATα* haploid strains are unsuitable for a mutational screen because only ~60% of all colonies with this genotype form filaments. To avoid this variability, we ectopically expressed the *PHD1* gene, an enhancer of filamentation (GIMENO and FINK 1994), in the *MAT***a**/*MATα* haploid strain we had constructed. These strains display greater homogeneity in colony morphology: filamentous growth on SLAD occurs at a frequency comparable to that of *MAT***a**/*MATα* diploid strains (>99% of the colonies form filaments). *PHD1* enhances filamentation only in the *MAT***a**/*MATα* haploids; haploids that are not heterozygous at the mating type locus (Figure 1) are not induced to form filaments by overexpression of *PHD1*.

Isolation of mutants defective for filamentous growth: To isolate *dfg*$^-$ mutants, we used a *MAT***a**/*MATα* haploid (strain 10511-9D; *MAT***a** *ura3-52 leu2::hisG trp1::hisG*) carrying both the *MATα* locus on a *URA3*-marked centromere plasmid and *PHD1* on a *TRP1*-marked 2 μm plasmid. This strain was mutagenized by integrative transformation with a transposon-mutagenized genomic library carrying random *Tn3::LEU2* gene insertions (Figure 2A; BURNS *et al.* 1994). Independent Leu$^+$ transformants (280,000) were collected and plated on nitrogen starvation (SLAD) medium. After 4 days of growth, 100,000 colonies were screened visually

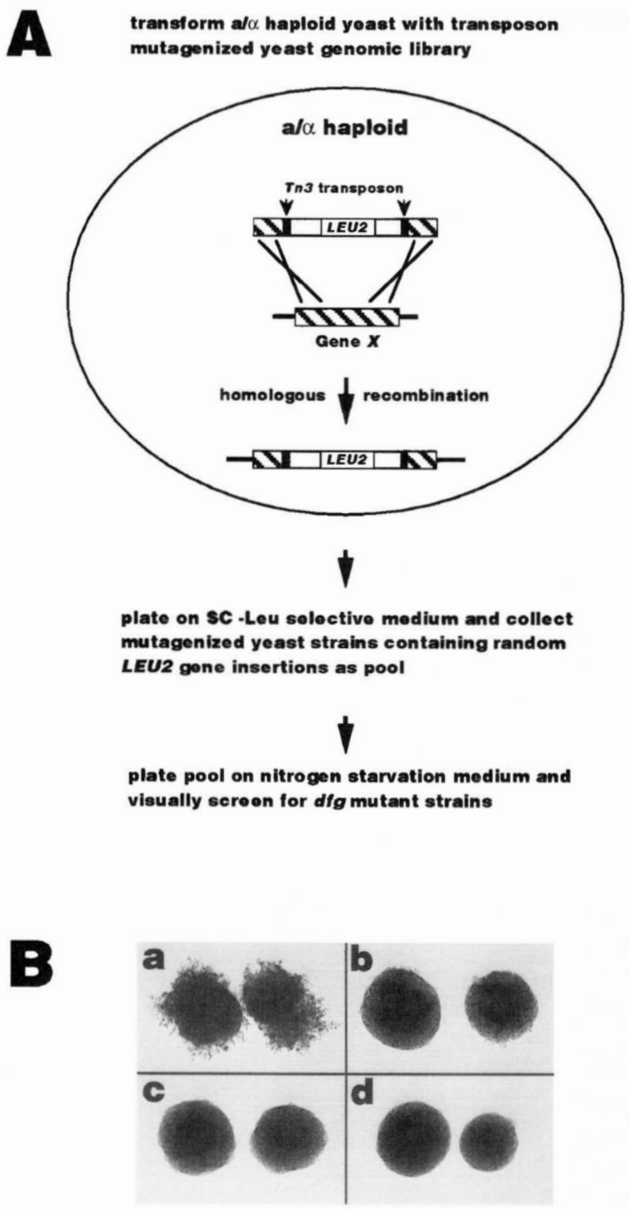

FIGURE 2.—Isolation of mutants defective for filamentous growth (*dfg*) in *MAT***a**/*MATα* haploid cells. (A) Outline of DFG screen. A *MAT***a**/*MATα* haploid strain (for details see MATERIALS AND METHODS) was transformed with a genomic library that had been mutagenized with *Tn3* transposon flanked *LEU2* gene insertions (BURNS *et al.* 1994). A pool of 280,000 independent Leu$^+$ transformants, consisting of mutants where random genomic loci *X* had been replaced with transposon mutagenized loci by homologous recombination events, was collected and plated on nitrogen starvation (SLAD) medium. After 4 days, 100,000 colonies were screened visually for mutants unable to form pseudohyphal filaments. (B) Filamentous growth defects of *MAT***a**/*MATα* haploid *dfg* mutant strains. Strains L5526 (a), and *dfg* mutant strains HMY15-248 (*ste12-101*) (b), HMY15-64 (*whi3-100*) (c), and HMY15-33 (*cdc39-100*), all carrying both plasmids B3364 (*PHD1* on 2 μm) and B2185 (*MATα* on a centromere plasmid) were patched on SC −Ura −Trp medium, grown overnight at 30°, and streaked to obtain single cells on nitrogen starvation (SLAD) medium. Plates were incubated at 30° and representative colonies were photographed after 72 hr of growth.

for mutants unable to form pseudohyphal filaments. Upon retesting, 56 Dfg$^-$ strains were identified that exhibited severe defects in filamentous growth (Figure 2B). A combination of genetic and molecular analysis was then performed on all 56 *dfg* mutants.

Segregants that had lost the plasmids carrying *PHD1* and the *MATα* locus were isolated from each putative mutant. These segregants were crossed to strain 10480-2C (*MATα ura3-52 leu2::hisG*). Five out of 56 Dfg$^-$ strains were sterile and were directly analyzed by rescue of the genomic DNA immediately adjacent to the *LEU2* insertion responsible for the mutation. DNA analysis revealed that these five sterile *dfg* mutants had transposon insertions at three different sites in the *STE12* gene (Table 3). *STE12* function is required for both filamentous growth and mating (LIU *et al.* 1993). The remaining 51 Dfg$^-$ strains were analyzed by tetrad analysis, and diploid strains either homozygous (by mating of ascospore progeny) or heterozygous for the insertion mutations were constructed and tested for filamentous growth (for details see MATERIALS AND METHODS). The *LEU2* marker from the insertion segment and a filamentous growth defect were genetically linked in 45 *dfg* mutants. In the remaining six Dfg$^-$ strains, the *dfg* mutations were not linked to the *LEU2* marker gene and were not analyzed further. Genomic DNA flanking the *LEU2* insertion was isolated from each of the remaining 45 *dfg* mutants and sequenced. This combination of genetic and molecular analysis revealed that the 45 mutants represent at least 35 independent mutational events, identifying 16 genes required for filamentous growth: *CDC39, STE12, TEC1, WHI3, NAB1, DBR1, CDC55, SRV2, TPM1, SPA2, BNI1, DFG5, DFG9, DFG10, BUD8* and *DFG16* (Table 3).

The *dfg* mutations define four classes: We characterized each of the diploid *dfg* mutants with respect to their ability to control the position of the bud site (CP, cell polarity), change in shape (CE, cell elongation) and ability to invade agar (INV, invasion). Bud site selection patterns were determined by staining bud scars of exponentially growing yeast form (YF) cells with calcofluor and dividing them into three groups: bipolar, random and unipolar (Figure 3A; Table 4). Substrate invasion was measured by determining the ratio of invasive *vs.* noninvasive cells of *dfg* mutants after growth on SLAD (Figure 3B; Table 4). The shape of invasive cells was then determined by defining three morphological groups: long PH cells, oval YF cells, and round YF cells (Figure 3C; Table 4; see MATERIALS AND METHODS). Characterization of all *dfg* mutants by these criteria defines four different classes (Table 4).

Class I (CP$^+$ CE$^-$ INV$^-$): Mutants in class I are impaired both for switching from the YF to the PH cell morphology and substrate invasion in response to nitrogen starvation, but have no defect in the budding pattern of the YF cells. Mutations in seven genes, *STE12, TEC1, CDC39, NAB1, WHI3, DBR1,* and *CDC55,* fall into

TABLE 3

Molecular and genetic analysis of *dfg* mutants

Gene	Reference	Mutant allele	Site of insertion[a]	Filamentation of homozygous mutant[b]
	Standard Σ diploid		No insertion	+++
CDC39	COLLART and STRUHL (1993)	*cdc39-100*	ORF (+3845)	–
STE12	ERREDE and AMMERER (1989)	*ste12::LEU2*		+/–
		ste12-100	Prom (−180)	ND
		ste12-101	Prom (−45)	ND
		ste12-102	ORF (+125)	ND
TEC1	LALOUX *et al.* (1990)	*tec1-100*	ORF (+145)	+
		tec1-101	ORF (+395)	+/–
WHI3	GenBank accession U01095	*whi3-100*	Prom (−275)	–
		whi3-101	ORF (+35)	ND
		whi3-102	ORF (+200)	ND
		whi3-103	ORF (+1205)	–
NAB1	GenBank accession M88277	*nab1-100*	Prom (−70)	–
DBR1	CHAPMAN and BOEKE (1991)	*dbr1-100*	ORF (+605)	+/–
CDC55	HEALY *et al.* (1991)	*cdc55-100*	Prom (−735)	–
SRV2	FIELD *et al.* (1990)	*srv2-100*	ORF (+725)	–
		srv2-101	ORF (+1340)	–
		srv2-102	ORF (+1400)	–
TPM1	LIU and BRETSCHER (1989)	*tpm1-100*	ORF (+40)	–
SPA2	GEHRUNG and SNYDER (1990)	*spa2-100*	ORF (+2985)	+
BNI1	GenBank accession L31766	*bni1-100*	ORF (+1520)	–
DFG5	PIR accession S57605, hypothetical protein YM9959.20	*dfg5-100*	Prom (−50)	–
		dfg5-101	ORF (+110)	+/–
DFG9	Swiss Prot accession P40091, hypothetical protein YEX9 or YER149C	*dfg9-100*	ORF (+365)	+
DFG10	Swiss Prot accession P40526, hypothetical protein YIE9 or YIL049W	*dfg10-100*	Prom (−20)	–
BUD8	GenBank accession L37016	*bud8-100*	Prom (−565)	–
		bud8-101	Prom (−375)	–
		bud8-102	Prom (−245)	–
		bud8-103	Prom (−25)	–
		bud8-104	ORF (+195)	–
		bud8-105	ORF (+320)	–
		bud8-106	ORF (+400)	–
		bud8-107	ORF (+450)	–
		bud8-108	ORF (+610)	–
		bud8-109	ORF (+670)	–
		bud8-110	ORF (+735)	–
DFG16	PIR accession S54363, hypothetical protein YOL303.14	*dfg16-100*	ORF (+1265)	+

ND, not detected.

[a] Approximate position (within 25 bp) of *Tn3::LEU2* insertions in the promoter region (Prom) or the protein coding region (ORF) are given relative to the translational start site ATG at position +1.

[b] Filamentation was assayed on nitrogen starvation (SLAD) plates, with control strain L5366 exhibiting a value of +++. For genes with only one mutant allele at least three homozygous and two heterozygous mutant strains were constructed from independent haploid spores. All alleles were recessive for filamentation defect (*whi3-101, whi3-102, ste12-100, ste12-101, ste12-102* were not determined).

this class. Mutations in *WHI3, CDC39,* and *CDC55* result in a strong defect in invasion, cell elongation, and filament formation. After 3 days of growth on nitrogen starvation medium, *whi3/whi3, cdc39/cdc39,* or *cdc55/cdc55* diploid colonies are virtually devoid of long cells and show no agar invasion (Figure 3B). The few cells remaining in the agar after the plates were washed are not organized into filaments. Mutations in the other four class I genes, *TEC1, STE12, NAB1* and *DBR1,* exhibit somewhat milder defects. Although diploid *tec1/tec1, ste12/ste12, nab1/nab1,* and *dbr1/dbr1* mutant strains do not develop visible filaments, these strains are leaky and develop some invasive filaments beneath the colonies after the surface growth has been removed by washing the plates. However, these filaments consist of cells with mostly YF morphology. In summary, the

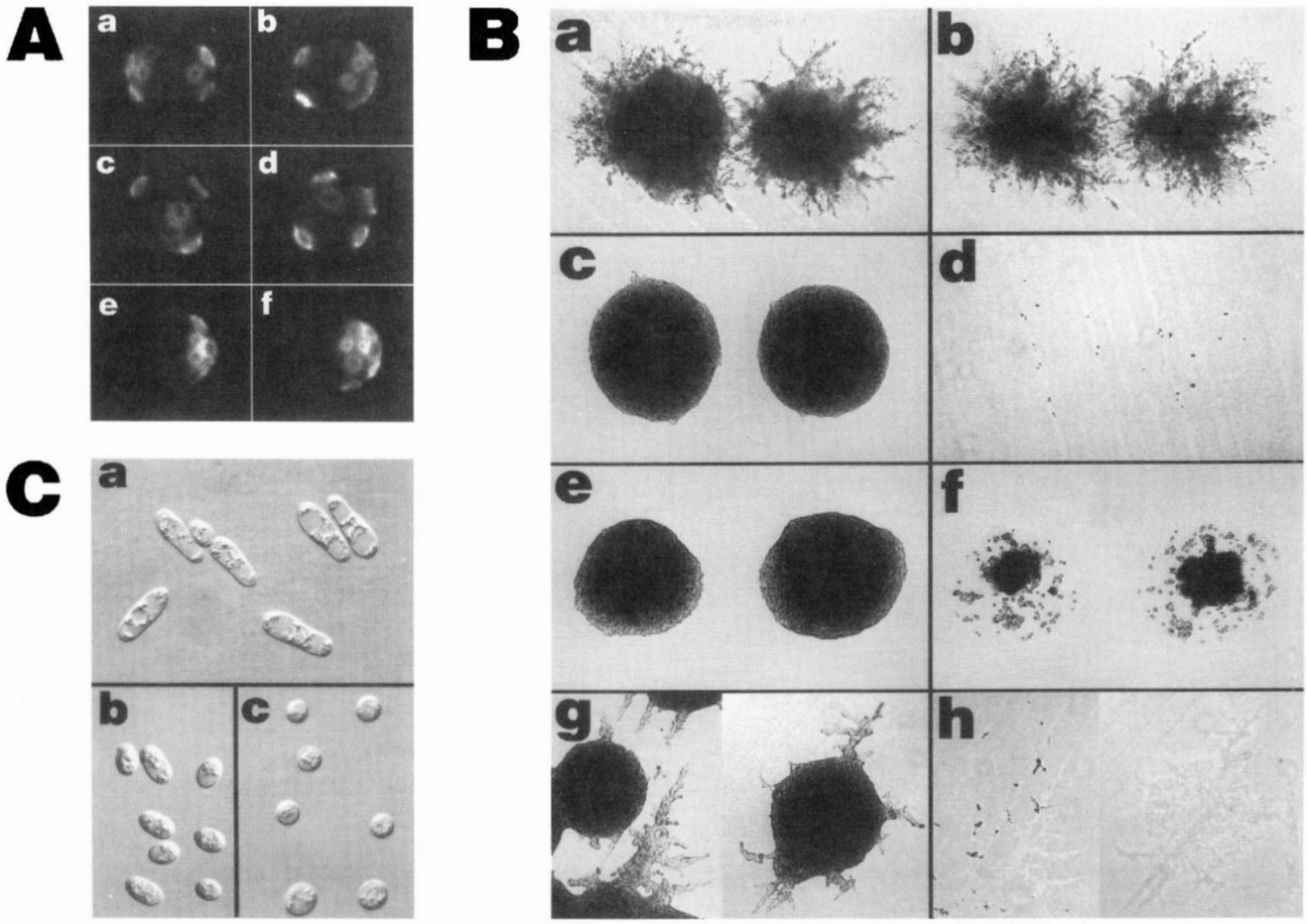

FIGURE 3.—Phenotypic analysis of *dfg* mutant strains. (A) Bud site selection patterns. Bud scars were stained and visualized for exponentially growing strains L5366 (a), HMC267 (*tec1-101/tec1-101*) (b), HMC281 (*tpm1-100/tpm1-100*) (c), HMC283 (*bni-100/bni1-100*) (d), HMC209 (*bud8-108/bud8-108*) (e), and HMC211 (*bud8-109/bud8-109*) (f), and representative cells are shown for bipolar (a and b), random (c and d) and unipolar (e and f) bud scar distribution. (B) Substrate invasion phenotypes. Strains L5366 (a and b), HMC233 (*whi3-100/whi3-100*) (c and d), HMC281 (*tpm1-100/tpm1-100*) (e and f), and HMC225 (*dfg16-100/dfg16-100*) (g and h) were patched on YPD medium, grown overnight at 30°, and streaked to obtain single cells on nitrogen starvation (SLAD +Ura) medium. Plates were incubated for 72 hr at 30°. Representative colonies were photographed before (a, c, e, and g) and after (b, d, f, and h) washing the plates. (C) Cell morphology phenotypes. Strains L5366, L5427 (*ste12::LEU2/ste12::LEU2*), and HMC281 (*tpm1-100/tpm1-100*) (c) were grown on nitrogen starvation (SLAD +Ura) medium for 72 hr and washed with water. Cells that had invaded the agar substrate were scraped out, dissolved in water and visualized under the microscope with Nomarski optics. Representative cells are shown for the long pseudohyphal (L5366) (a), oval (L5427) (b), and round yeast form morphology (HMC281) (c).

phenotypic appearance of class I mutants, intact morphology and polarity in their YF, but failure to respond to nitrogen starvation, suggests a role for class I genes in signaling for filamentous growth. Sequence analysis of class I genes also predicts a function in cell signaling or gene regulation. *STE12* (DOLAN *et al.* 1989; ERREDE and AMMERER 1989; YUAN and FIELDS 1991), *TEC1* (LALOUX *et al.* 1990, 1994), and *CDC39* (COLLART and STRUHL 1993, 1994) all encode known transcription factors. In addition, *TEC1* has been reported to be required for filamentous growth in *S. cerevisiae* (GAVRIAS *et al.* 1996). *NAB1* is a gene with unknown function, but its gene product was localized to the nucleus (Genbank accession M88277). The predicted amino acid sequence of *WHI3* (Genbank accession U01095) includes a motif found in known RNA binding proteins. *DBR1* is required for intron turnover (CHAPMAN and BOEKE 1991) and *CDC55* encodes the regulatory subunit for protein phosphatase 2A (HEALY *et al.* 1991).

Class II (CP^- CE^- INV^+): Mutants in class II are defective in cell polarity and cell elongation, but still invade the agar. Seven genes were identified that belong to this class, *TPM1, SPA2, BNI1, SRV2, DFG5, DFG9* and *DFG10.* Mutations in these genes lead to random budding patterns, indicative of severe cell polarity defects (Table 4). Moreover, class II mutants are round YF cells (Table 4), irrespective of their nutritional status, demonstrating a role in regulation of cell morphology. The specific function of class II genes in cell polarity and morphogenesis was further corroborated by analysis of their sequence. *TPM1* codes for the major form of tropomyosin in yeast and is a component of the microfil-

TABLE 4

Classification of *dfg* mutants

Class	Strain	Relevant genotype	Budding pattern			Invasion	Cell shape		
			Bipolar (%)	Random (%)	Unipolar (%)		Long PH (%)	Oval YF (%)	Round YF (%)
Standard	L5366		73	7	20	+++	18	73	9
Class I	HMC203	*cdc39-100/cdc39-100*	87	9	4	+	0	21	79
	L5427	*ste12::LEU2/ste12::LEU2*	72	9	19	+	3	74	23
	HMC267	*tec1-101/tec1-101*	71	4	25	+	2	69	29
	HMC233	*whi3-100/whi3-100*	67	15	18	−	0	4	96
	HMC275	*nab1-100/nab1-100*	50	12	38	+	0	44	56
	HMC237	*dbr1-100/dbr1-100*	62	10	28	+	6	54	40
	HMC199	*cdc55-100/cdc55-100*	39	49	12	+	0	19	81
Class II	HMC205	*srv2-100/srv2-100*	18	82	0	−	0	1	99
	HMC281	*tpm1-100/tpm1-100*	14	85	1	++	0	2	98
	HMC245	*spa2-100/spa2-100*	30	67	3	++	0	22	78
	HMC283	*bni1-100/bni1-100*	15	75	10	++	0	7	93
	HMC235	*dfg5-100/dfg5-100*	36	35	29	++	0	7	93
	HMC263	*dfg9-100/dfg9-100*	7	85	8	++	0	6	94
	HMC239	*dfg10-100/dfg10-100*	14	84	2	++	0	6	94
Class III	HMC209	*bud8-108/bud8-108*	28	5	67	++	18	59	23
Class IV	HMC225	*dfg16-100/dfg16-100*	75	5	20	−	19	53	28

ament cytoskeleton (LIU and BRETSCHER 1989). *SPA2* encodes a structural protein that is required for projection formation during mating and colocalizes with actin to shmoo tips (GEHRUNG and SNYDER 1990). In addition, *SPA2* has recently been demonstrated to be required for the bipolar bud site selection program (ZAHNER *et al.* 1996). *BNI1,* identified originally because the *bni1* mutation is synthetically lethal in combination with a *cdc12* mutation (FARES and PRINGLE, as cited in MARHOUL and ADAMS 1995), is required for the bipolar bud site selection pattern (ZAHNER *et al.* 1996) and has been found to be required for mother cell-specific *HO* expression (BOBOLA *et al.* 1996; JANSEN *et al.* 1996). *SRV2* codes for adenylyl cyclase associated protein (Srv2p or CAP) and is known to be important for the organization of the actin cytoskeleton (FIELD *et al.* 1990; GERST *et al.* 1991). Moreover, Srv2p interacts with actin and actin-interacting proteins *in vivo* and *in vitro* (AMBERG *et al.* 1995; FREEMAN *et al.* 1995, 1996). *DFG5, DFG9* and *DFG10* were sequenced as part of the Yeast Genome Project, and code for three predicted proteins YM9959.20, YER149c and YIL049w, respectively, that share no homology to any protein in the data base. As none of these ORFs had previously been assigned a function, we have renamed them *DFG5, DFG9* and *DFG10* (Table 3).

All class II mutants (except *srv2* mutants) were still able to invade the agar substrate upon nitrogen starvation. For example, a *tpm1/tpm1* diploid strain is unable to form filaments of PH cells when growing on SLAD, but agar invasion is intact (Figure 3B). Thus, class II mutants separate cell polarity and morphogenesis from invasive growth, suggesting that invasion may involve a distinct pathway.

Class III (CP^- CE^+ INV^+): Mutations in class III fail to elaborate the unipolar budding pattern required for the formation of linear filaments, but do not affect cell elongation or substrate invasion. Although there is only one gene, *BUD8,* in this class, we isolated 11 different *bud8* mutant alleles each of which exhibits the identical phenotype. *BUD8* is required for distal bud site selection (the site opposite to the birth end of the cell) in YF cells (ZAHNER *et al.* 1996). Using time lapse photography, we found that *bud8/bud8* mutants bud with a very high frequency from the proximal pole (at the birth end of the cell) whether on rich medium (Table 3 and Table 4) or growing on nitrogen starvation conditions (SLAD, data not shown). The inability of *bud8/bud8* mutants to bud from the distal pole explains their inability to form filaments. When grown on SLAD, *bud8/bud8* strains form PH cells and invade the agar (Table 4), demonstrating that morphology and invasion are genetically separable from bud site selection.

Class IV (CP^+ CE^+ INV^-): Mutants in class IV are defective in invasion, but do not affect cell polarity or filament formation. *DFG16,* the one gene in this class, was sequenced as part of the Yeast Genome Project but, as no function had been assigned to it, we renamed it. The predicted amino acid sequence of *DFG16* does not show homology to other known proteins. When grown on nitrogen starvation medium, *dfg16/dfg16* mutants (Figure 3B) produce filaments of long PH cells, albeit with a slightly reduced frequency. However, the filaments do not invade the agar, and can be easily removed from the surface by washing the plate. The existence of the *dfg16/dfg16* mutant phenotype further supports the proposition that invasion is a genetically distinct function from cell polarity and morphogenesis.

In summary, the phenotypic analysis of *dfg* mutant strains combined with DNA sequence analysis of *DFG* genes suggests that the switch from YF growth to PH growth requires several different processes, each of which is under distinct genetic control.

Interactions between *DFG* genes and elements of the filamentous growth signaling pathway: Filamentous growth is controlled by an evolutionarily conserved signaling pathway in which Ras2p signals via the Cdc42p/Ste20p/MAPK module (MÖSCH *et al.* 1996). To identify putative targets of this signal transduction pathway that account for the changes in cell polarity, cell elongation and invasive growth, we tested epistasis between *dfg* mutations and gain-of-function mutations in *RAS2* (*RAS2^{Val19}*), *STE11* (*STE11-4*) and *STE12* (overexpression plasmid containing *STE12*). As these alleles of *RAS2, STE11,* and *STE12* cause enhanced filamentous growth (GIMENO *et al.* 1992; LIU *et al.* 1993; Table 5), they are referred to as "filamentous growth enhancers." Diploid *dfg* mutant strains were first transformed with different plasmids containing either the *RAS2^{Val19}* or *STE11-4* mutant alleles or with a high copy plasmid that results in overexpression of *STE12.* Double mutants composed of a *dfg* mutation and a gain-of-function mutation were analyzed for their phenotypes (summarized in Table 5).

Expression of the filamentous growth enhancers allowed us to group class I genes into four different subclasses:

Mutations in both *CDC39* and *CDC55* severely block filamentous growth enhancement by *RAS2^{Val19}* (~12-fold by *cdc39-100* and about sixfold by *cdc55-100*), but only weakly block enhancement by *STE11-4* (roughly twofold by both *cdc39-100* and *cdc55-100*). This result suggests that both *CDC39* and *CDC55* might function downstream of *RAS2* but upstream of *STE11.*

Mutations in *STE12* or *TEC1* completely block the filamentous growth enhancement by *STE11-4,* and partially block the enhancement by *RAS2^{Val19}.* Thus, *STE12* as well as *TEC1* appear to act downstream of both *STE11* and *RAS2.* Furthermore, overexpression of Tec1p does not suppress the filamentous growth defect of a *ste12* mutant, and reciprocally, overexpression of Ste12p does not suppress the *tec1* mutant phenotype (Table 6; Figure 4), suggesting that the transcription factors Ste12p and Tec1p may interact to regulate filamentous growth. This observation agrees with our previous work, which showed that both *STE12* and *TEC1* are required for the expression of the same transcriptional reporter, a finding that was interpreted to meant that Ste12p might bind in concert with Tec1p to promote transcription of genes required for filamenous growth (MÖSCH *et al.* 1996). In addition, mutations in both *TEC1* and *STE12* block the enhancement of filamentous growth by Phd1p to the same degree (Table 6; Figure 4), again suggesting a synergistic role for Tec1p and Ste12p.

whi3 mutations completely block filamentous growth even in the presence of *RAS2^{Val19}* or *STE11-4,* or when *STE12* was overexpressed, suggesting a role for *WHI3* downstream of *STE12.* The filamentous growth phenotypes of *nab1* and *dbr1* are partially suppressed by both *RAS2^{Val19}* and *STE11-4,* indicating a role for *NAB1* and *DBR1* upstream of or parallel to the filamentous growth signaling pathway.

Class II genes encode structural components of the actin cytoskeleton or the bud neck filaments and are likely downstream targets of the filamentous growth enhancers. As expected, the PH morphogenesis defects of six of the seven class II mutants (*srv2, tpm1, spa2, bni1, dfg5* and *dfg9*) are not suppressed by *RAS2^{Val19}, STE11-4* or high copy *STE12.* The remaining class II mutant, *dfg10,* is partially suppressed only by *RAS2^{Val19}.*

The cell polarity defect of a *bud8* mutant (class III) is not suppressed by any of the pseudohyphal enhancers. However, loss of *BUD8* function did not block the enhancement of cell elongation by *RAS2^{Val19}* or *STE11-4,* showing that cell elongation is distinct from the bud site selection process.

The invasive growth defect of a *dfg16* mutant (class IV) could not be suppressed by *RAS2^{Val19}* nor by *STE11-4* or high copy levels of *STE12,* indicating that the invasion defect of *dfg16* lies downstream of the filamentous growth signaling pathway. By contrast, the number and length of filaments, as well as PH cell morphogenesis of a *dfg16/dfg16* mutant strain were still enhanced by *RAS2^{Val19}* and by *STE11-4,* showing that the *DFG16* defect is restricted to invasive growth.

DISCUSSION

Transposon mutagenesis combined with the complete *S. cerevisiae* genome sequence data is a fast and efficient screening tool: Our procedure for obtaining mutants defective in filamentation circumvents the problem that filamentation is a diploid phenotype; recessive mutations affecting the phenotype cannot be detected in the diploids. There are methods that permit the isolation of mutations in diploid-specific traits. For example, mutations that block meiotic sporulation were isolated using homothallic yeast strains, which express the *HO* gene (ESPOSITO and ESPOSITO 1969; HERSKOWITZ and JENSEN 1991). These protocols are based on the idea that, after mutagenesis, haploids expressing Ho switch mating type within the clone to produce haploid strains of opposite mating type, and thus will mate to produce homozygous diploids expressing the mutant phenotype. As an alternative, we found that expression of *MATα* from a plasmid in a *MAT***a** haploid strain gave a sufficiently diploid-like filamentation phenotype that we could use these haploid strains for the mutant screen. Moreover, after loss of the *MATα* plasmid, the mutations could be analyzed by straightforward backcrosses.

A second feature of our procedure is the use of a *Tn3* transposon insertion library as the mutagenic

TABLE 5

Effects of different pseudohyphal enhancers in *dfg* mutants

Class	Strain	Relevant genotype		Invasion	Cell shape		
		Chromosome	Plasmid		Long PH (%)	Oval YF (%)	Round YF (%)
Standard	L5366		Vector	+++	18	73	9
			RAS2^{Val19}	++++	49	47	4
			STE11-4	++++	45	48	7
			STE12 2μm	++++	29	66	5
Class I	HMC203	*cdc39-100/cdc39-100*	Vector	+	0	21	79
			RAS2^{Val19}	++	4	73	23
			STE11-4	++	23	69	8
			STE12 2μm	++	14	48	38
	L5427	*ste12::LEU2/ste12::LEU2*	Vector	+	3	74	23
			RAS2^{Val19}	++	17	62	21
			STE11-4	+	3	78	19
			STE12 2μm	+++	28	71	1
	HMC267	*tec1-101/tec1-101*	Vector	+	2	69	29
			RAS2^{Val19}	++	12	64	24
			STE11-4	+	4	63	33
			STE12 2μm	+	3	61	36
	HMC233	*whi3-100/whi3-100*	Vector	−	0	4	96
			RAS2^{Val19}	+	0	39	61
			STE11-4	−	0	9	91
			STE12 2μm	−	0	7	93
	HMC275	*nab1-100/nab1-100*	Vector	+	0	44	56
			RAS2^{Val19}	+++	16	70	14
			STE11-4	+++	25	64	11
			STE12 2μm	++	14	63	23
	HMC237	*dbr1-100/dbr1-100*	Vector	+	6	54	40
			RAS2^{Val19}	+++	19	71	10
			STE11-4	+++	21	51	28
			STE12 2μm	++	14	64	22
	HMC199	*cdc55-100/cdc55-100*	Vector	+	0	19	81
			RAS2^{Val19}	++	8	73	19
			STE11-4	++	24	57	19
			STE12 2μm	+	9	76	15
Class II	HMC205	*srv2-100/srv2-100*	Vector	−	0	1	99
			RAS2^{Val19}	+	0	9	91
			STE11-4	−	0	4	96
			STE12 2μm	−	0	3	97
	HMC281	*tpm1-100/tpm1-100*	Vector	++	0	2	98
			RAS2^{Val19}	+++	0	15	85
			STE11-4	+++	0	10	90
			STE12 2μm	+++	0	11	89
	HMC245	*spa2-100/spa2-100*	Vector	++	0	22	78
			RAS2^{Val19}	+++	1	62	37
			STE11-4	+++	1	29	70
			STE12 2μm	+++	0	26	74
	HMC283	*bni1-100/bni1-100*	Vector	++	0	7	93
			RAS2^{Val19}	+++	0	26	74
			STE11-4	+++	0	21	79
			STE12 2μm	++	0	17	83
	HMC235	*dfg5-100/dfg5-100*	Vector	+	0	7	93
			RAS2^{Val19}	+++	2	21	77
			STE11-4	+++	0	15	85
			STE12 2μm	++	0	21	79
	HMC263	*dfg9-100/dfg9-100*	Vector	++	0	6	94
			RAS2^{Val19}	+++	0	28	72
			STE11-4	+++	0	13	87
			STE12 2μm	+++	0	9	91

TABLE 5

Continued

Class	Strain	Relevant genotype: Chromosome	Relevant genotype: Plasmid	Invasion	Cell shape: Long PH (%)	Cell shape: Oval YF (%)	Cell shape: Round YF (%)
Class II	HMC239	*dfg10-100/dfg10-100*	Vector	+	0	6	94
			RAS2^{Val19}	+++	13	41	46
			STE11-4	++	5	39	56
			STE12 2μm	++	0	5	95
Class III	HMC209	*bud8-108/bud8-108*	Vector	++	18	59	23
			RAS2^{Val19}	+++	36	60	4
			STE11-4	+++	30	55	15
			STE12 2μm	+++	21	48	31
Class IV	HMC225	*dfg16-100/dfg16-100*	Vector	−	19	53	28
			RAS2^{Val19}	+	42	56	2
			STE11-4	−	31	60	9
			STE12 2μm	−	26	62	12

agent. This protocol has two major advantages over chemical or UV mutagenesis. First, transposon insertion mutations are genetically tagged with a selectable marker and thus, during genetic analysis, can be easily followed in haploid strains that do not express diploid-specific phenotypes. Second, genetically-tagged mutant alleles can be directly cloned by a two step rescue procedure and sequenced from a unique site in the transposon, providing immediate identification of the disrupted locus (BURNS *et al.* 1994). The availability of the entire yeast genomic sequence means that only minimal sequencing is required for gene identification and location of the insertion within the gene. We have found that mutagenesis by the transformation/isolation procedure is efficient, although transformation itself appears to be somewhat mutagenic. Six of the 56 *dfg* mutations were not linked to the *LEU2* insertion. Of course, another intrinsic problem is that mutations in genes encoding vital functions are not likely to be isolated.

Our screen did not recover several genes known to affect filamentous growth including *RAS2, CDC42, STE20, STE11* and *STE7* (GIMENO *et al.* 1992; LIU *et al.* 1993; MÖSCH *et al.* 1996). There are several possible explanations for the absence of these mutations. (1) The screen was not performed to saturation. (2) The insertion element *Tn3* does not insert randomly. (3) *Tn3* insertions in essential genes such as *CDC42* cannot be recovered. Probably all three explanations are relevant in our study. An additional reason for not recovering upstream signaling genes such as *RAS2, CDC42, STE20, STE11* or *STE7* could be that the presence of *PHD1* on a 2 μm plasmid either partially or completely suppresses the filamentation defects of these mutants.

Invasion is distinct from filamentation: We identified 16 genes, comprising four different classes, that dissect filamentous growth into distinct cellular processes. A key finding is that invasion is genetically separable from the morphogenetic processes of cell elongation (CE)

TABLE 6

***STE12, TEC1* and *PHD1* interactions**

Strain	Relevant genotype: Chromosome	Relevant genotype: Plasmid	Invasion	Cell shape: Long PH (%)	Cell shape: Oval YF (%)	Cell shape: Round YF (%)
L5366		Vector	+++	18	73	9
		STE12 2 μm	++++	29	66	5
		TEC1 2 μm	++++	31	66	3
		PHD1 2 μm	++++	55	45	0
L5427	*ste12::LEU2/ste12::LEU2*	Vector	+	3	74	23
		STE12 2 μm	++++	28	71	1
		TEC1 2 μm	+	7	84	9
		PHD1 2 μm	+++	23	74	3
HMC267	*tec1-101/tec1-101*	Vector	+	2	69	29
		STE12 2 μm	+	3	61	36
		TEC1 2 μm	++++	30	65	5
		PHD1 2 μm	+++	15	76	9

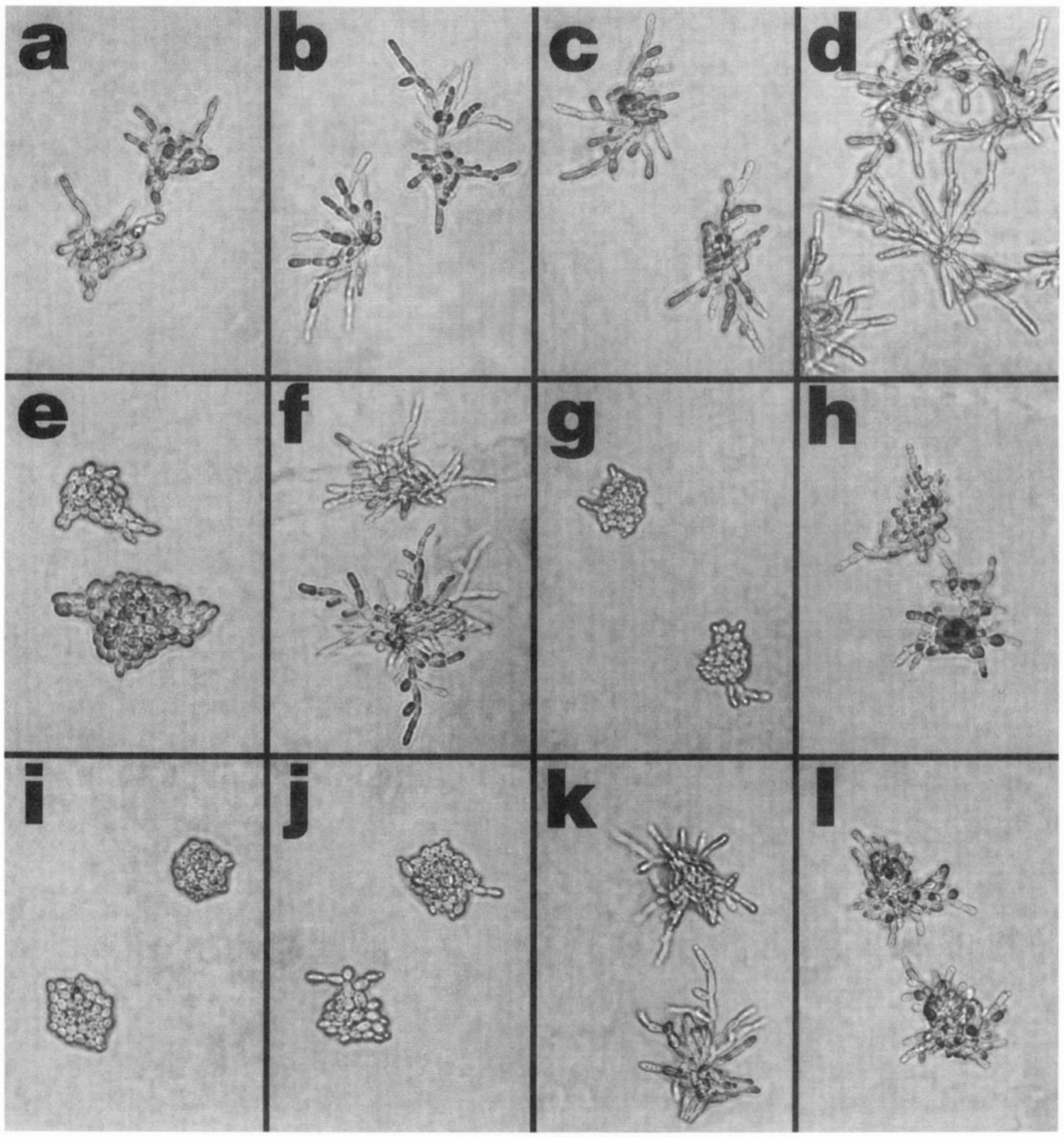

FIGURE 4.—Genetic interactions between *STE12, TEC1* and *PHD1* during filamentous growth. Strains L5366 (wild type) (a–d), L5427 (*ste12::LEU2/ste12::LEU2*) (e–h), and HMC267 (*tec1-101/tec1-101*) (i–l) carrying either plasmid pRS316 (a, e, and i), B2065 (2 μM *STE12*) (b, f, and j), B3366 (2 μm *TEC1*) (c, g, and k), or pCG38 (2 μm *PHD1*) (d, h, and l) were patched on SC −Ura medium, grown overnight at 30°, and streaked to obtain single cells on nitrogen starvation (SLAD) medium. Plates were incubated at 30° and representative colonies were photographed after 18 hr.

and bud site selection (CP). Class II mutants exhibit CP^- and CE^- phenotypes but are Inv^+, whereas the class IV mutant *dfg16/dfg16* is CP^+ and CE^+, but Inv^-. Moreover, bud site selection can be separated from invasion (and cell elongation), because *bud8/bud8* mutants are CP^-, but Inv^+ and CE^+. These results suggest the existence of a specific invasion pathway that includes *DFG16* and is a target of the filamentous growth signaling pathway (Figure 5). The fact that mutations in *STE12,* as well as *STE20, STE11* and *STE7* (ROBERTS and FINK 1994), cause a defect in invasion, argues for a model where this invasion pathway is a downstream target of the Ste12p signaling pathway. Such a model is further supported by the finding that overexpression of Ste12p does not suppress the Inv^- phenotype of a *dfg16/dfg16* mutant. However, an alternative model, where *DFG16* is part of a pathway required for invasion that acts in parallel to the filamentous growth signaling pathway, cannot be ruled out.

PH cell morphogenesis requires genes controlling the actin cytoskeleton, bud neck filament assembly and cell asymmetry: We uncovered mutations in several genes, *BNI1, SPA2, TPM1,* and *SRV2,* that are required for the formation of long pseudohyphal cells. These genes

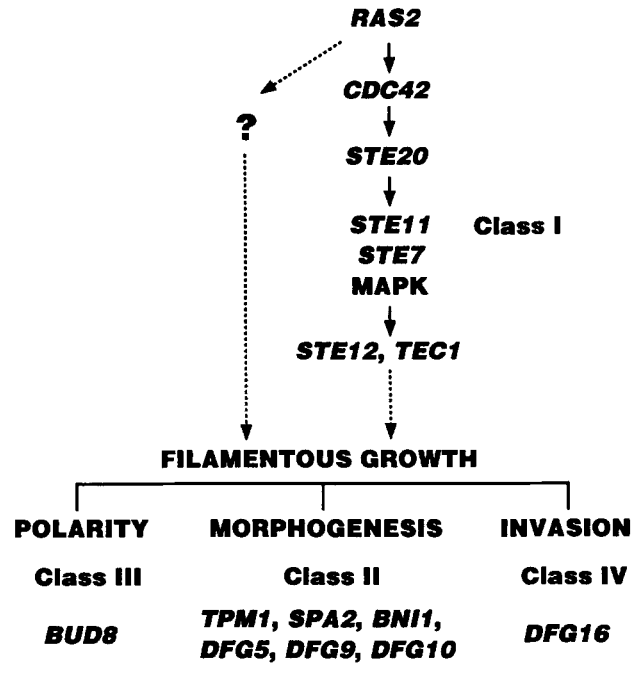

FIGURE 5.—Model for filamentous growth development in *S. cerevisiae*. The model reflects the genetic dissection of filamentous growth by mutations in different classes of *DFG* genes into the cellular processes of signal transduction (class I), bud site selection (polarity; class III), morphogenesis (class II) and invasive growth (invasion; class IV). The putative regulation of class II, class III and class IV genes by the signal transduction molecules encoding genes of class I is indicated by dotted arrows. Signaling of Ras2p via the Cdc42p/Ste20p/MAPK module during filamentous growth has been demonstrated (MÖSCH *et al.* 1996). Activation of filamentous growth by *RAS2* via an yet unknown parallel pathway is indicated by a question mark and is based on the finding that mutations in *STE20, STE11, STE7, STE12* and *TEC1* only partially suppress filamentous growth enhancement by dominant active $RAS2^{Val19}$ (MÖSCH *et al.* 1996; and Table 5 of this manuscript).

encode structural components known to interact with the actin cytoskeleton or bud neck filaments. Previous work had shown that PH cells (in contrast with YF cells) maintain a polarized actin cytoskeleton throughout bud growth, suggesting an important role of actin and actin-interacting proteins in the regulation of PH cell morphogenesis (KRON *et al.* 1994).

Our finding that both *bni1* and *spa2* mutants are completely suppressed for cell elongation indicates that components essential for cytokinesis and bud shape are also required for the cellular differentiation of filamentous fungi. *bni1* was originally identified as a mutation that is synthetic lethal in combination with a mutation in *CDC12* (FARES and PRINGLE, as cited in MARHOUL and ADAMS 1995), a gene that encodes a septin required for cytokinesis and bud shape (LONGTINE *et al.* 1996). Moreover, a *bni1* null mutation significantly affects the structure of the bud neck and produces a partial defect in cytokinesis, indicating interaction of Bni1p with the bud neck filament proteins (FARES and PRINGLE, as cited in MARHOUL and ADAMS 1995). This view of Bni1p function is supported by studies in other fungi. In *Candida albicans*, homologues of the *S. cerevisiae CDC3* and *CDC10* genes are expressed at higher levels in hyphal cells than in YF cells (DI DOMENICO *et al.* 1994), suggesting a role for septins in hyphal formation. In *Aspergillus nidulans*, overexpression of *figA*, a gene with 42% identity to *BNI1*, has been shown to alter the shape of hyphal cells (MARHOUL and ADAMS 1995). The importance of cell separation in PH growth is emphasized by our finding that a *spa2* mutation suppresses PH cell elongation. *SPA2*, like *BNI1*, has been implicated in neck filament assembly (FLESCHER *et al.* 1993), again suggesting an important role for this protein and septins in pseudohyphal morphogenesis.

The first cell division in the formation of the pseudohyphal filament is asymmetric; a round mother divides to form a long, thin pseudohyphal daughter. The finding that both Tpm1p, the major form of tropomyosin in yeast, and Bni1p are required for filament formation is intriguing because these proteins have been implicated in other cell asymmetries. In yeast *HO*-induced mating type switch is asymmetric; mothers can switch, but daughters must wait a generation. Bni1p, together with the minimyosin Myo4p, is required for asymmetric accumulation of the Ash1p repressor of *HO* gene expression in daughter cell nuclei at the end of mitosis. (BOBOLA *et al.* 1996; JANSEN *et al.* 1996). In Drosophila oocytes, the accumulation of *oskar* mRNA at the posterior end of the egg depends upon tropomyosin (ERDELYI *et al.* 1995), suggesting that actin cytoskeletal components play an important role in the unequal segregation of developmental determinants. The fact that Tpm1p, the major form of tropomyosin in yeast, and Bni1p are required for PH morphogenesis suggests that the formation of filaments in *S. cerevisiae* may depend on the asymmetric distribution of as yet unknown pseudohyphal developmental factors.

We thank MICHAEL SNYDER for kindly providing the transposon mutagenized yeast genomic DNA library. We thank CARLOS GIMENO, PETER HECHT, STEVE KRON and other members of the Fink lab for many fruitful discussions and BRIAN CALI, TODD MILNE, STEFFEN RUPP and ERIC SUMMERS for helpful comments on the manuscript. This work was supported by National Institutes of Health research grant GM-40266 to G.R.F. H.-U.M. was supported by postdoctoral fellowships of the Swiss National Science Foundation (SNF) and of the International Human Frontier Science Program Organization (H.F.S.P.O). G.R.F. is an American Cancer Society Professor of Genetics.

LITERATURE CITED

ALTSCHUL, S. F., W. GISH, W. MILLER, E. W. MYERS and D. J. LIPMAN, 1990 Basic local alignment search tool. J. Mol. Biol. **215:** 403–410.

AMBERG, D. C., E. BASART and D. BOTSTEIN, 1995 Defining protein interactions with yeast actin *in vivo*. Nat. Struct. Biol. **2:** 28–35.

BANUETT, F., 1992 *Ustilago maydis*, the delightful blight. Trends Genet. **8:** 174–178.

BLACKETER, M. J., C. M. KOEHLER, S. G. COATS, A. M. MYERS and P. MADAULE, 1993 Regulation of dimorphism in *Saccharomyces cerevisiae:* involvement of the novel protein kinase homolog Elm1p and protein phosphatase 2A. Mol. Cell. Biol. **13:** 5567–5581.

BOBOLA, N., R.-P. JANSEN, T. H. SHIN and K. NASMYTH, 1996 Asymmetric accumulation of Ash1p in postanaphase nuclei depends on a myosin and restricts yeast mating-type switching to mother cells. Cell **84:** 699–709.

BURNS, N., B. GRIMWADE, P. B. ROSS-MACDONALD, E. Y. CHOI, K. FINBERG *et al.*, 1994 Large-scale analysis of gene expression, protein localization, and gene disruption in *Saccharomyces cerevisiae.* Genes Dev. **8:** 1087–1105.

CHAPMAN, K. B., and J. D. BOEKE, 1991 Isolation and characterization of the gene encoding yeast debranching enzyme. Cell **65:** 483–492.

COLLART, M. A., and K. STRUHL, 1993 Cdc39, an essential nuclear protein that negatively regulates transcription and differentially affects the constitutive and inducible *HIS3* promoters. EMBO J. **12:** 177–186.

COLLART, M. A., and K. STRUHL, 1994 *NOT1(CDC39), NOT2(CDC36), NOT3,* and *NOT4* encode a global-negative regulator of transcription that differentially affects TATA-element utilization. Genes Dev. **8:** 525–537.

DI DOMENICO, B. J., N. H. BROWN, J. LUPISELLA, J. R. GREENE, M. YANKO *et al.*, 1994 Homologs of the yeast neck filament associated genes: isolation and sequence analysis of *Candida albicans CDC3* and *CDC10.* Mol. Gen. Genet. **242:** 689–698.

DOLAN, J. W., C. KIRKMAN and S. FIELDS, 1989 The yeast Ste12 protein binds to the DNA sequence mediating pheromone induction. Proc. Natl. Acad. Sci. USA **86:** 5703–5707.

ERDELYI, M., A. M. MICHON, A. GUICHET, J. B. GLOTZER and A. EPHRUSSI, 1995 Requirement for Drosophila cytoplasmic tropomyosin in oskar mRNA localization. Nature **377:** 524–7.

ERREDE, B., and G. AMMERER, 1989 Ste12, a protein involved in cell-type-specific transcription and signal transduction in yeast, is part of protein-DNA complexes. Genes Dev. **3:** 1349–1361.

ESPOSITO, M. S., and R. E. ESPOSITO, 1969 The genetic control of sporulation in Saccharomyces. I. The isolation of temperature-sensitive sporulation-deficient mutants. Genetics **61:** 79–89.

FIELD, J., A. VOJTEK, R. BALLESTER, G. BOLGER, J. COLICELLI *et al.*, 1990 Cloning and characterization of CAP, the *S. cerevisiae* gene encoding the 70 kd adenylyl cyclase-associated protein. Cell **61:** 319–327.

FLESCHER, E. G., K. MADDEN and M. SNYDER, 1993 Components required for cytokinesis are important for bud site selection in yeast. J. Cell Biol. **122:** 373–386.

FREEMAN, N. L., Z. CHEN, J. HORENSTEIN, A. WEBER and J. FIELD, 1995 An actin monomer binding activity localizes to the carboxyl-terminal half of the *Saccharomyces cerevisiae* cyclase-associated protein. J. Biol. Chem. **270:** 5680–5685.

FREEMAN, N. L., T. LILA, K. A. MINTZER, Z. CHEN, A. J. PAHK *et al.*, 1996 A conserved proline-rich region of the *Saccharomyces cerevisiae* cyclase-associated protein binds SH3 domains and modulates cytoskeletal localization. Mol. Cell. Biol. **16:** 548–556.

FREIFELDER, D., 1960 Bud position in *Saccharomyces cerevisiae.* J. Bacteriol. **80:** 567–568.

GAVRIAS, V., A. ANDRIANOPOULOS, C. J. GIMENO and W. E. TIMBERLAKE, 1996 *Saccharomyces cerevisiae TEC1* is required for pseudohyphal growth. Mol. Microbiol. **19:** 1255–1263.

GEHRUNG, S., and M. SNYDER, 1990 The *SPA2* gene of *Saccharomyces cerevisiae* is important for pheromone-induced morphogenesis and efficient mating. J. Cell Biol. **111:** 1451–1464.

GERST, J. E., K. FERGUSON, A. VOJTEK, M. WIGLER and J. FIELD, 1991 CAP is a bifunctional component of the *Saccharomyces cerevisiae* adenylyl cyclase complex. Mol. Cell. Biol. **11:** 1248–1257.

GIETZ, D., J. A. ST. JEAN, R. A. WOODS and R. H. SCHIESTL, 1992 Improved method for high efficiency transformation of intact yeast cells. Nucleic Acids Res. **20:** 1425.

GIMENO, C. J., and G. R. FINK, 1992 The logic of cell division in the life cycle of yeast. Science **257:** 626.

GIMENO, C. J., and G. R. FINK, 1994 Induction of pseudohyphal growth by overexpression of *PHD1,* a *Saccharomyces cerevisiae* gene related to transcriptional regulators of fungal development. Mol. Cell. Biol. **14:** 2100–2112.

GIMENO, C. J., P. O. LJUNGDAHL, C. A. STYLES and G. R. FINK, 1992 Unipolar cell divisions in the yeast *S. cerevisiae* lead to filamentous growth: regulation by starvation and *RAS.* Cell **68:** 1077–1090.

GRENSON, M., M. MOUSSET, J. M. WIAME and J. BECHET, 1966 Multiplicity of the amino acid permeases in *S. cerevisiae.* Biochim. Biophys. Acta **127:** 325–338.

HEALY, A. M., S. ZOLNIEROWICZ, A. E. STAPLETON, M. GOEBL, A. A. DE PAOLI-ROACH *et al.*, 1991 *CDC55,* a *Saccharomyces cerevisiae* gene involved in cellular morphogenesis: identification, characterization, and homology to the B subunit of mammalian type 2A protein phosphatase. Mol. Cell. Biol. **11:** 5767–5780.

HERSKOWITZ, I., and R. E. JENSEN, 1991 Putting the *HO* gene to work: practical uses for mating-type switching. Methods Enzymol. **194:** 132–146.

HOFFMAN, C. S., and F. WINSTON, 1987 A ten-minute DNA preparation from yeast efficiently releases autonomous plasmids for transformation of *Escherichia coli.* Gene **57:** 267–272.

ITO, H., Y. FUKUDA, K. MURAI and A. CHIMERA, 1983 Transformation of intact yeast cells treated with alkali actions. J. Bacteriol. **153:** 163–168.

JANSEN, R.-P., C. DOWSER, C. MICHAEL'S, M. GLOVE and K. NASMYTH, 1996 Mother cell-specific *HO* expression in budding yeast depends on the unconventional Myo4p and other cytoplasmic proteins. Cell **84:** 687–697.

KRON, S. J., C. A. STYLES and G. R. FINK, 1994 Symmetric cell division in pseudohyphae of the yeast *Saccharomyces cerevisiae.* Mol. Biol. Cell **5:** 1003–1022.

LALOUX, I., E. DUBOIS, M. DEWERCHIN and E. JACOBS, 1990 *TEC1,* a gene involved in the activation of Ty1 and Ty1-mediated gene expression in *Saccharomyces cerevisiae:* cloning and molecular analysis. Mol. Cell. Biol. **10:** 3541–3550.

LALOUX, I., E. JACOBS and E. DUBOIS, 1994 Involvement of SRE element of Ty1 transposon in *TEC1*-dependent transcriptional activation. Nucleic Acids Res. **22:** 999–1005.

LIU, H., C. A. STYLES and G. R. FINK, 1993 Elements of the yeast pheromone response pathway required for filamentous growth of diploids. Science **262:** 1741–1744.

LIU, H. P., and A. BRETSCHER, 1989 Disruption of the single tropomyosin gene in yeast results in the disappearance of actin cables from the cytoskeleton. Cell **57:** 233–242.

LJUNGDAHL, P. O., C. J. GIMENO, C. A. STYLES and G. R. FINK, 1992 *SHR3:* a novel component of the secretory pathway specifically required for localization of amino acid permeases in yeast. Cell **71:** 463–478.

LONGTINE, M. S., D. J. DE MARINI, M. L. VALENCIK, O. S. AL-AWAR, H. FARES *et al.*, 1996 The septins: roles in cytokinesis and other processes. Curr. Opin. Cell Biol. **8:** 106–119.

MARHOUL, J. F., and T. H. ADAMS, 1995 Identification of developmental regulatory genes in *Aspergillus nidulans* by overexpression. Genetics **139:** 537–547.

MERSON-DAVIES, L. A., and F. C. ODDS, 1989 A morphology index for characterization of cell shape in *Candida albicans.* J. Gen. Microbiol. **135:** 3143–3152.

MÖSCH, H.-U., R. L. ROBERTS and G. R. FINK, 1996 Ras2 signals via the Cdc42/Ste20/mitogen-activated protein kinase module to induce filamentous growth in *Saccharomyces cerevisiae.* Proc. Natl. Acad. Sci. USA **93:** 5352–5356.

ODDS, F. C., 1987 Candida infections: an overview. Crit. Rev. Microbiol. **15:** 1–5.

ODDS, F. C., 1992 Candida infections in AIDS patients [editorial]. Int. J. Std. Aids **3:** 157–160.

ROBERTS, R. L., and G. R. FINK, 1994 Elements of a single MAP kinase cascade in *Saccharomyces cerevisiae* mediate two developmental programs in the same cell type: mating and invasive growth. Genes Dev. **8:** 2974–2985.

SCHULZ, B., F. BANUETT, M. DAHL, R. SCHLESINGER, W. SCHAFER *et al.*, 1990 The *b* alleles of *U. maydis,* whose combinations program pathogenic development, code for polypeptides containing a homeodomain-related motif. Cell **60:** 295–306.

SHEPHERD, M. G., 1988 Morphogenetic transformation of fungi. Curr. Top. Med. Mycol. **2:** 278–304.

SHERMAN, F., G. R. FINK and J. HICKS, 1986 *Methods in Yeast Genetics.* Cold Spring Harbor Laboratory Press, Cold Spring Harbor, NY.

YUAN, Y. L., and S. FIELDS, 1991 Properties of the DNA-binding domain of the *Saccharomyces cerevisiae* Ste12 protein. Mol. Cell. Biol. **11:** 5910–5918.

ZAHNER, J. E., H. A. HARKINS and J. R. PRINGLE, 1996 Genetic analysis of the bipolar pattern of bud site selection in the yeast *Saccharomyces cerevisiae.* Mol. Cell. Biol. **16:** 1857–1870.

Communicating editor: M. D. ROSE